CONSORTIUM for BUILDING ENERGY INNOVATION

REPORT

Title: **Virtual RTU Sensing Automation, Demonstration, and Assessment**

Report Date: **April 30, 2016**

Report Authors: **Akash Patil, Andrew L. Hjortland, James E. Braun**

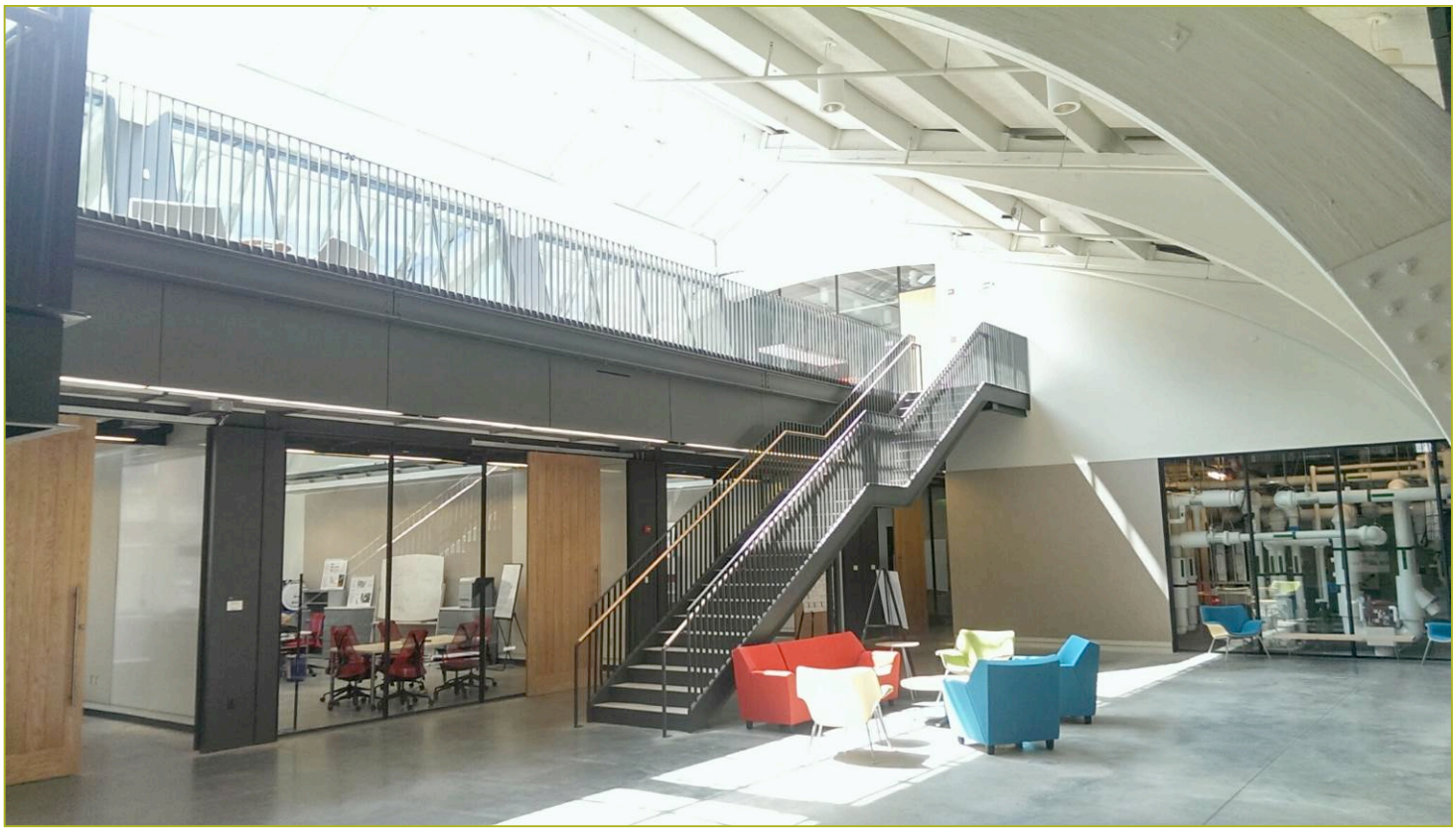

Funded by U.S. DOE

Report Abstract

This report describes validation and documentation of an automated system for training virtual refrigerant charge sensors for rooftop unit air conditioners along with an overall assessment of virtual sensor implementation requirements and performance. The system automatically tunes empirical parameters of a virtual sensor for estimating the amount of refrigerant in a system. The engineering time and costs associated with calibrating a virtual sensor are reduced because of the automated testing, a reduction in the number of tests required, and because the training is accomplished using open laboratory testing rather within psychrometric chambers. In order to assess the accuracy of this approach, the system was applied to four different RTUs (with varying types of components). The outputs of models trained using the open laboratory automated training kit were compared with data collected for the units tested within psychrometric chamber test facilities over a wide range of ambient conditions. The results showed that the virtual refrigerant charge sensor models had root-mean-square errors less than 10%. This shows that the automated open laboratory training system results in accurate sensors for many types of RTUs.

Contact Information for lead researcher

Name: James E. Braun
Institution: Purdue University
Email address: jbraun@purdue.edu
Phone number: 765-494-9157

Contributors

Akash Patil, Andrew L. Hjortland, Orkan Kurtulus, James E. Braun – Purdue University

Contents

1. Introduction

1.1. Project Motivation and Objectives

Studies have shown that RTUs tend to be poorly maintained and significant energy may be wasted annually due to unnoticed or unrepaired equipment faults. Previous work on fault detection and diagnostics (FDD) for HVAC systems has demonstrated positive results and potential for significant energy and utility cost savings associated with identifying faults in these systems sooner. This is especially true of virtual sensor based FDD protocols because of the ability to detect and diagnose multiple faults simultaneously.

Despite the promising results obtained by previous work on FDD, manufacturers have been slow to incorporate FDD technologies for a few reasons:

- FDD systems must be low-cost and easy to install,
- uncertainty with respect to economic benefit/savings potential still exists,
- and lack of integration and interoperability with other building technologies.

In order to address these issues, a suite of virtual sensors have been designed within a low-cost microprocessor using only temperature (or pressure) measurements. These virtual sensors include a virtual refrigerant charge sensor, virtual cooling capacity sensor, and virtual COP sensor. This designed system includes plans for all hardware and software requirements. Ultimately, this virtual sensor package can be integrated within a RTU FDD system to provide an extensive fault detection and diagnostics capability. The virtual charge sensor has been designed to estimate the amount of refrigerant charge in a direct-expansion air conditioner and relies on empirical parameters that must be determined using system performance data collected in a laboratory setting. The training requirement can be costly if psychrometric chamber test facilities are required to collect the necessary data. To reduce this cost, an automated methodology that tunes the empirical parameters of the Virtual Refrigerant Charge (VRC) sensor in an open laboratory space has been developed and the accuracy of using this method is presented in this report.

1.2. Virtual Sensors

Recent research has provided evidence that fault detection sensitivity and fault diagnosis accuracy of fault detection and diagnostics (FDD) methodologies can be improved when accurate virtual sensor technologies are incorporated without adding significant instrumentation costs. One advantage of virtual sensors is the ability to estimate physical quantities that may be too expensive to measure directly. Furthermore, some quantities like the amount of refrigerant charge contained in a direct-expansion (DX) air-conditioning system are impossible to measure directly while the unit is in operation. Previous work has shown units that are undercharged tend to have less available cooling capacity and tend to operate with lower efficiency. One additional advantage of virtual sensors is the ability to

decouple HVAC equipment components so that different virtual sensors are only sensitive to a single fault. This enables accurate fault diagnoses even when multiple faults affect a system simultaneously.

Virtual Refrigerant Charge Sensor

Previous work has shown that the amount of refrigerant charge contained in a system can be estimated using measurements of the compressor suction superheat and liquid-line subcooling. The compressor suction superheat, ΔT_{sh}, is equal to the temperature difference defined by Equation (1.1)

$$\Delta T_{sh} = T_{suc} - T_{eri} \tag{1.1}$$

where T_{suc} is the refrigerant temperature at the compressor inlet (suction) and T_{eri} is the temperature of the refrigerant entering the evaporator (a measure of saturation temperature). The liquid-line subcooling, ΔT_{sc}, is calculated using a similar temperature difference, given by Equation (1.2),

$$\Delta T_{sc} = T_{crs} - T_{cro} \tag{1.2}$$

where T_{crs} is the refrigerant saturation temperature in the condenser and T_{cro} is the refrigerant temperature at the condenser outlet. The amount of refrigerant charge in a DX system relative to the normal amount can be estimated using a virtual refrigerant charge sensor. The functional form of this sensor is given by Equation (1.3)

$$\frac{m_{\text{actual}} - m_{\text{normal}}}{m_{\text{normal}}} = k_{sh}\left(\Delta T_{sh} - \Delta T_{sh,rated}\right) + k_{sc}\left(\Delta T_{sc} - \Delta T_{sc,rated}\right) + k_x\left(x_{eri} - x_{eri,rated}\right) \tag{1.3}$$

where $\Delta T_{sh,rated}$, $\Delta T_{sc,rated}$, and $x_{eri,rated}$ are the superheat, subcooling, and evaporator refrigerant inlet quality of a properly charged system at the rating condition, respectively. Equation (1.3) also requires three empirical parameters: k_{sh}, k_{sc}, k_x. Determining these empirical parameters using performance data collected in an open laboratory space was described previously in Milestone Report 2.5.a.

The correlation defined by Equation (1.3) requires the thermodynamic quality of the refrigerant entering the evaporator. Since it is impossible to measure the thermodynamic quality directly, the use of thermodynamic property relations and a commonly used vapor-compression cycle assumption must be used to estimate this quantity. Commonly, the expansion process of the vapor compression cycle is assumed to be isenthalpic; the enthalpy at the inlet and outlet of the expansion valve is constant,

$$h_{cro} = h_{eri}. \tag{1.4}$$

With this assumption, the thermodynamic quality at the evaporator inlet, x_{eri}, can be calculated using thermodynamic property relations if the condenser outlet enthalpy is known and the evaporator inlet temperature is measured,

$$x_{eri} = f(T_{eri}, h_{eri} = h_{cro}). \tag{1.5}$$

To calculate the enthalpy of the enthalpy of the refrigerant exiting the condenser, thermodynamic property relations can be used when nonzero subcooling exists using the outlet temperature and the condenser saturation temperature.

Virtual Compressor Power Sensor

Some faults, especially faults reducing the condenser airflow or heat transfer coefficient like fouling, have a significant impact on the instantaneous power drawn by the compressor. An FDD algorithm can detect these problems when abnormal power is drawn by the system. While direct measurements of compressor power are available, these are relatively expensive when compared with the typical cost of a RTU. A virtual compressor power sensor has been developed using low-cost temperature measurements as an alternative to direct power sensor measurements.

This virtual sensor is essentially a performance mapping of the compressor power under different operating conditions. These mappings are actually available for all compressors used in air-conditioning applications since it is required by the Air-Conditioning, Heating, and Refrigeration Institute (AHRI), a certification organization. This means no additional laboratory tests are required to train empirical parameters since compressor manufacturers must perform them and make the results available. A 10-coefficient polynomial equation is used to relate the compressor suction saturation temperature, T_{ers}, and the compressor discharge saturation temperature, T_{crs} , to the compressor power requirement, $\dot{W}_{map}$,

$$\begin{aligned}\dot{W}_{map} = a_0 + \\ a_1 T_{ers} + a_2 T_{crs} + \\ a_3 T_{ers}^2 + a_4 T_{ers} T_{crs} + a_5 T_{crs}^2 + \\ a_6 T_{ers}^3 + a_7 T_{ers}^2 T_{crs} + a_8 T_{ers} T_{crs}^2 + a_9 T_{crs}^3\end{aligned} \tag{1.6}$$

where $a_{0\ldots9}$ are empirical coefficients that can be obtained from a manufacturer's data sheet. When a compressor with multiple stages is used on the system, a set of empirical coefficients are required for each stage of operation. To evaluate the compressor map given by Equation (1.6), measurements of two-phase refrigerant temperature in the evaporator and condenser can be used (evaporator inlet and a condenser return bend temperature). If direct measurements of the saturation temperatures are not possible, suction and discharge pressure transducers can be used to calculate these saturation temperatures since pressure and temperature are dependent properties within the two-phase dome.

Virtual Refrigerant Mass Flow Rate Sensor

Another important and useful quantity that can be leveraged by FDD algorithms is the system refrigerant mass flow rate. The mass flow rate of refrigerant within the system is impacted by many faults and reductions in mass flow rate can lead to reductions in cooling capacity and cycle efficiency. Along with compressor power, AHRI also requires rating the mass flow rate through a compressor at different operating conditions. As before, a 10-coefficient polynomial correlation in terms of T_{ers} and T_{crs} are required by manufacturers to relate the mass flow rate, $\dot{m}_{map}$,

$$\begin{aligned}\dot{m}_{map} = a_0 + \\ a_1 T_{ers} + a_2 T_{crs} +\end{aligned} \tag{1.7}$$

$$a_3 T_{ers}^2 + a_4 T_{ers} T_{crs} + a_5 T_{crs}^2 + a_6 T_{ers}^3 + a_7 T_{ers}^2 T_{crs} + a_8 T_{ers} T_{crs}^2 + a_9 T_{crs}^3$$

where $a_{0\ldots9}$ are empirically determined coefficients. One limitation using Equation (1.7) to estimate refrigerant mass flow rate in practice is related to the superheat used when determining the empirical parameters. During the testing, superheat is held at a constant value. Unfortunately, this is not the case in an actual system, where variations in superheat are likely due to different expansion devices, ambient conditions, and charge levels. An additional adjustment must be made to the performance map output to account for differences between the actual suction superheat and the superheat maintained during the ratings process. A correlation is given by Dabiri and Rice (1981) to account for variations in actual suction superheat during actual compressor operation,

$$\dot{m}_{ref} = \left[1 + F\left(\frac{\rho_{rated}}{\rho_{actual}} - 1\right)\right] \dot{m}_{map} \tag{1.8}$$

where ρ_{actual} and ρ_{rated} are measurements of the actual and rated suction density and F is an empirical parameter usually set to 0.75. In order to determine the actual suction density, thermodynamic property relations are used along with measurements of the compressor suction state.

Virtual Cooling Capacity Sensor

Perhaps the most important impact on system performance that a fault has on an air-conditioning system is the impact on cooling capacity. When total cooling capacity is reduced, the system must run longer to meet a given load and consume more energy. Furthermore, if cooling capacity is reduced sufficiently, the air conditioner may not have enough capacity during times of high loads. To estimate the cooling capacity of an air-conditioning system, a virtual cooling capacity sensor has been proposed that relies on state point measurements at the inlet and outlet of the evaporator, as well as the refrigerant mass flow rate. By calculating the enthalpy at the evaporator inlet, h_{eri}, and the compressor suction, h_{suc}, the cooling capacity can be calculated using Equation (1.9),

$$\dot{Q}_{cool} = \dot{m}_{ref}(h_{suc} - h_{eri}) \tag{1.9}$$

where $\dot{m}_{ref}$ is the mass flow rate of refrigerant in the system (given by the virtual refrigerant mass flow rate sensor). Using Equation (1.9) along with a properly tuned FDD algorithm enables detection of faults that impact cooling capacity.

Virtual COP Sensor

A final measure of system performance for an air conditioning system is the coefficient of performance (COP), which is the ratio of total cooling capacity to total power consumption. This performance metric is effectively the efficiency of the system, which can be calculated at any time during operation. Because of this, it is convenient to have an estimate of the current system COP within a FDD tool. Equation (1. 10) describes a virtual sensor for COP in terms of the virtual cooling capacity and virtual compressor power sensors.

$$\mathrm{COP} = \frac{\dot{Q}_{cool}}{\dot{W}_{map}} \quad (1.\ 10)$$

By using the virtual COP sensor as part of a FDD package, degradation in cooling cycle performance can be measured and faults impacting system efficiency can be detected.

Virtual Sensor Implementation

The virtual sensors were implemented as part of a complete VOLTRON-compatible FDD system that is described in Deliverable D2.2.1. The prototype solution incorporates a BeagleBone Black circuit board and 6 thermistor temperature sensors. An initial cost assessment was performed (see Milestone Report 2.5.b) and it is estimated that a production virtual sensor unit that includes refrigerant charge, refrigerant mass flow rate, compressor power, cooling capacity, and COP could be manufactured at a cost of less than $40.

2. Description of Virtual Charge Sensor Training Kit Hardware

An overall schematic of the RTU components, the sensor measurements, the control variables, and the information flow for the virtual sensor training kit is shown in Figure 2.1. The hardware selected for the prototype is generally considered to be typical and relatively low-cost when compared to similar data acquisition applications within the HVAC market. The prototype was also designed to simplify assembly and debugging so a few components not typically found in an actual application are used, namely the solderless breadboard (which can easily be swapped with a more permanent through-hole perforated board or printed circuit board) and the microcontroller (pictured in Figure 2.2).

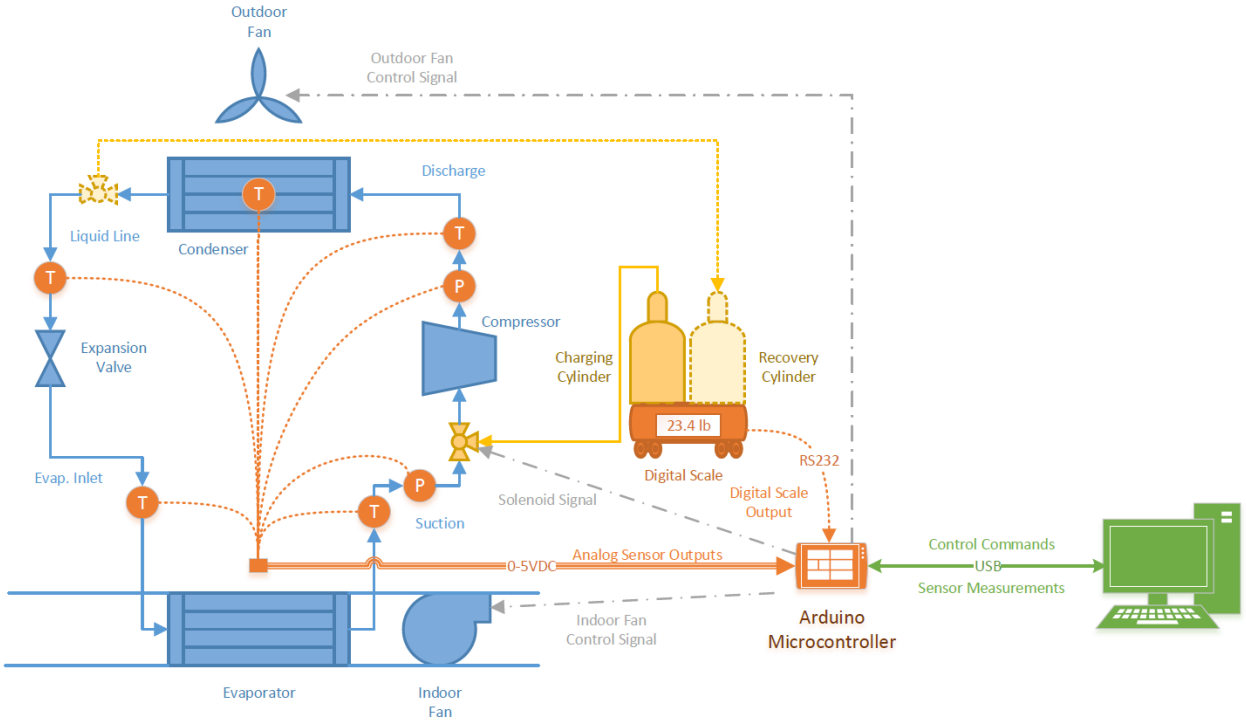

Figure 2.1. Overall schematic of the VRC sensor training kit developed to automate empirical model parameter tuning. The required sensors and arrows indicating the control variables are shown. The system requires a microcontroller to provide low-level monitoring and control and a personal computer to supervise the process. Note that in the initial implementation charge is only added to the system, but could also be removed by adding the liquid-line solenoid valve and a recovery tank pictured.

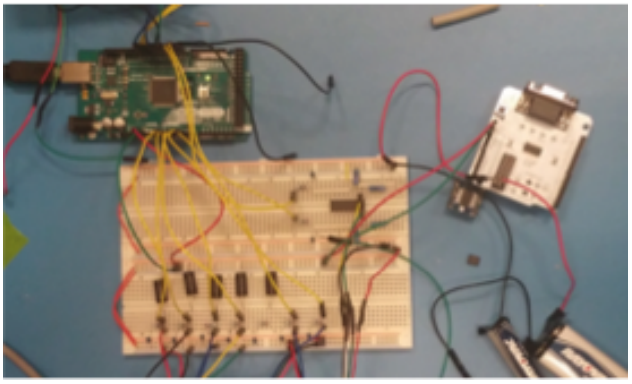

Figure 2.2. Initial virtual charge sensor training kit microcontroller hardware and electronics circuit prototype implementation.

After the prototype on breadboard was successful, the electronics was shifted to through hole plates with dedicated sensor circuits. Each plate had circuit dedicated to either pressure transducers or the temperature sensors. Figure 2.3 shows the implementation of the virtual charge sensor training kit using the through hole plates.

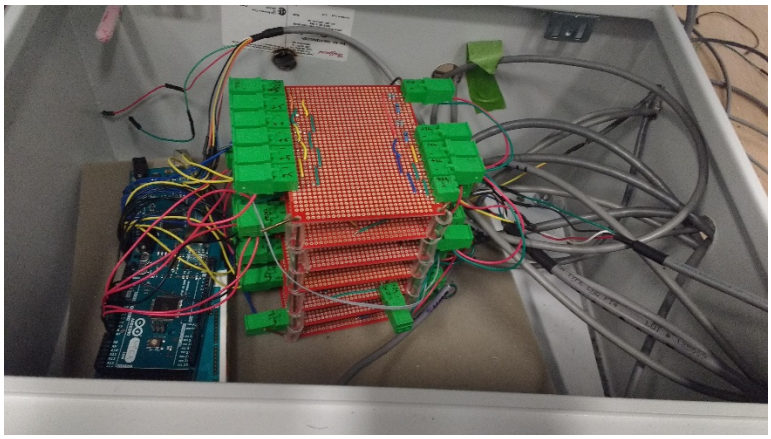

Figure 2.3. Virtual charge sensor training kit microcontroller hardware and electronics circuit implementation using through hole plates.

An Arduino Mega2560 microcontroller has been used to interface with the sensors and control interfaces required to implement the automated training algorithm. Compared to other microcontrollers, the Arduino development environment makes interfacing with sensors and digital outputs relatively easy and with little configuration. To enable this, the Arduino designers have developed an extension of the C++ programming language with built-in functions that can be used to read and write to the digital and analog input and outputs found on the microcontroller.

In order to implement the VRC training algorithm, several refrigerant-side temperature and pressure measurements are required, shown in Table 2.1. Using these sensors, the empirical parameters used in the VRC sensor can be tuned using the training algorithm. It should also be noted that pressure measurements can be used to calculate the evaporator refrigerant inlet temperature and condenser refrigerant saturation temperature since the refrigerant at these points is a two-phase fluid. Systems that already have these pressure sensors installed for control purposes do not need to install additional temperature sensors which reduces instrumentation costs. Pressure sensors may be required for systems with microchannel condensers since locating a reliable saturation temperature point is not trivial.

To measure these refrigerant-side temperatures, low-cost thermistor circuits were designed. This circuit was also used for the VOLTTRON™ RTU AFDD implementation in Project 2.2 and is described in Deliverable D2.2.1. This ensures that when the automated VRC training methodology is applied to the RTU, the empirical parameters are directly usable by the AFDD system. The thermistors selected for the application have to be surface-mounted to the RTU refrigerant circuit in the locations required. Compared to other types of temperature sensor types (thermocouples, RTDs, etc.) thermistors offer the best combination of accuracy, reliability, and cost. Pressure transducers have also been installed on the system considered in this study to measure the low- and high-side pressures. The high-side pressure is important for the RTU being tested since it has a microchannel condenser. This makes measuring the

condenser saturation temperature nearly impossible or unreliable with surface-mounted temperature sensors.

Table 2.1. Description of required refrigerant-side temperature measurements used for training the virtual refrigerant charge sensor.

Symbol	Type	Description
T_{eri} [1]	10 kΩ Thermistor	Evaporator Refrigerant Inlet Temperature
T_{suc}	10 kΩ Thermistor	Compressor Refrigerant Suction Temperature
T_{dis}	10 kΩ Thermistor	Compressor Refrigerant Discharge Temperature
T_{crs} [2]	10 kΩ Thermistor	Condenser Refrigerant Saturation Temperature
T_{cro}	10 kΩ Thermistor	Condenser Refrigerant Outlet Temperature
P_{suc}	0-300 PSIG Pressure Transducer	Compressor Refrigerant Suction Gauge Pressure
P_{dis}	0-500 PSIG Pressure Transducer	Compressor Refrigerant Discharge Gauge Pressure

[1] The evaporator refrigerant inlet temperature measurement can be replaced by the compressor suction pressure measurement when it is difficult or impossible to measure the evaporator inlet temperature accurately.

[2] The condenser refrigerant saturation temperature measurement can be replaced by the compressor discharge pressure measurement when it is difficult or impossible to measure the condenser saturation temperature accurately (due to a microchannel condenser, for example).

The hardware implementation also incorporates components used to control the operational mode of the RTU (shown in Figure 2.3) and the control set-points of the indoor fan and outdoor fan. The operational mode of the unit (controlling the system to stand-by, fan-only, low-stage cooling, or high-stage cooling mode) is controlled using a set of three relays. The relays are connected to the G, Y1, Y2 thermostat signals and are sequenced using the software implementation. Conventional control of the indoor and outdoor fans has been overridden using electronically commutated (EC) motor controllers producing a 0-10 VDC pulse-width-modulated output. The duty cycle of the controllers is controlled via the software implementation for each fan. The motor controlling the indoor fan provides a constant torque output so the PWM output provides the torque set-point of the motor. The outdoor fan is driven by a constant speed motor, thus the PWM output provides the speed setting to the motor. Figure 2.4 shows the initial installation of the relay control unit and EC motor controllers inside the compressor compartment of the RTU. The modules were installed within the compressor compartment for electrical safety precautions; when an external enclosure is designed and built these components will reside outside the unit.

Figure 2.3. RTU used to test automated VRC sensor training kit and evaluate performance of VRC sensor applied to RTU with different types of expansion valves and condenser coils.

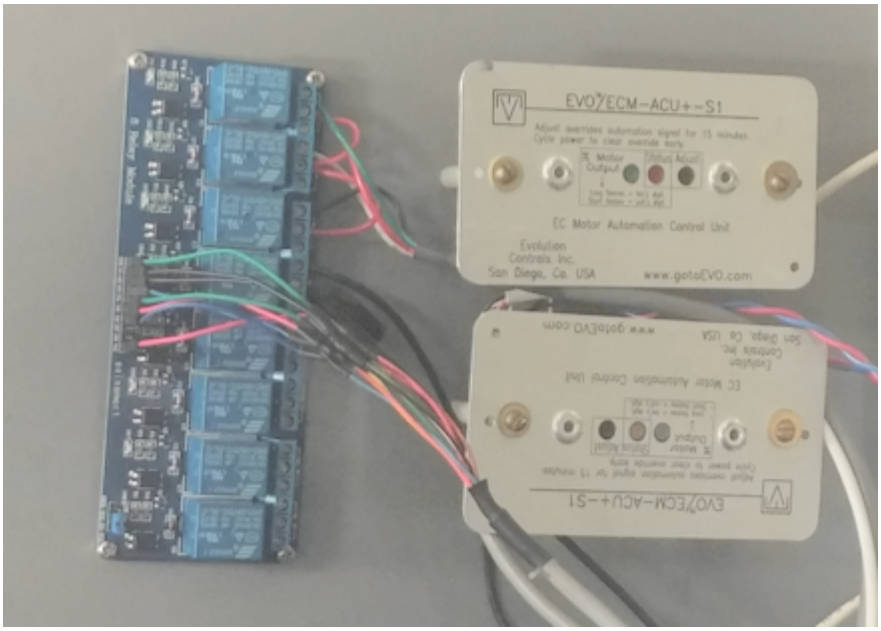

Figure 2.4. Installation of the relay control module and EC motor controller modules installed inside the RTU compressor compartment.

Refrigerant charge addition is automatically controlled using a suction-side solenoid valve and an electronic weighing scale with a digital output (shown in Figure 2.5). A relay is used to control the solenoid valve position from the microcontroller using a digital 5 VDC output. When the solenoid is open, refrigerant charge is able to enter the refrigerant circuit of the RTU. The refrigerant charging bottle is placed on the electronic scale in order to measure the mass of refrigerant that has left the cylinder and entered the refrigerant circuit. The personal computer interfaces with the digital output of the scale via a USB serial data connection.

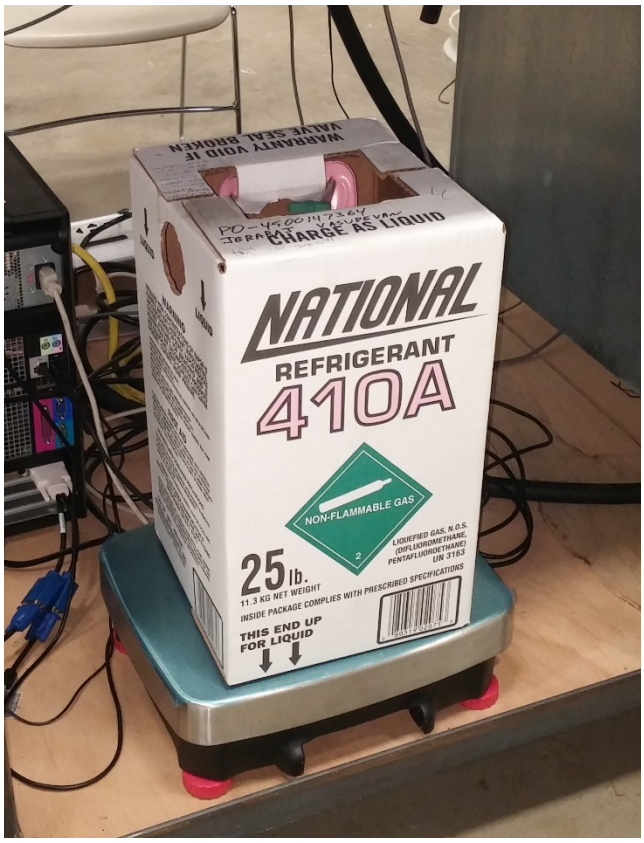

Figure 2.5. Digital weighing scale with refrigerant charging cylinder used to adjust the RTU charge level automatically.

The last component of the automated VRC sensor training kit is a personal computer that is used to run the Python software implementation of the automated training algorithm. A USB serial data connection is use to interface the personal computer and the microcontroller. The software on the personal computer uses logic to determine the control outputs and collects the required sensor outputs used for tuning the empirical VRC parameters.

3. Description of Automated Training Kit Software

An implementation of the VRC sensor training algorithm has been created using open-source software packages. As previously noted, the training kit is comprised of one microcontroller and one personal computer each performing different functions. The software embedded on the microcontroller is implemented using the Arduino variant of the C++ programming language. The software used on the personal computer is implemented using the Python programming language. These two systems communicate between one another via a USB data connection.

3.1. Microcontroller Software Implementation Details

On the microcontroller side, the software is implemented so that when a control input sequence is received, the following sequence is performed:

1. ***Receive control input sequence.***
   The last process performed by the microcontroller is to send the measured sensor values back to the personal computer via USB serial connection. The output string takes the following form:

   ```
                MODE     IDF      ODF     ADD_CHRG   REM_CHRG
          [    {-},     {%},     {%},      {-},       {-},     ]
   ```

   where

MODE:	RTU Operating Mode, [-1, 0, 1, 2]
IDF:	Indoor Fan Torque Setting, [0, 1, …, 100]
ODF:	Outdoor Fan Speed Setting, [0, 1, …, 100]
ADD_CHRG:	Low-side Solenoid Valve Position, [0, 1]
REM_CHRG:	High-side Solenoid Valve Position, [0, 1].

2. ***Update cooling mode.***
   This routine is used to set the desired cooling state of the RTU by activating relays connected to the RTU thermostat signal input. There are four possible states:

-1:	System OFF	(G: 0, Y1: 0, Y2: 0)
0:	Fan Only Mode	(G: 1, Y1: 0, Y2: 0)
1:	Low Cooling Mode	(G: 1, Y1: 1, Y2: 0)
2:	High Cooling Mode	(G: 1, Y1: 1, Y2: 1).

   Each thermostat signal has a dedicated relay with an input controlled by a digital output on the microcontroller.

3. ***Update fan control set-points.***
   This routine is used to control the two RTU fans to the desired torque and speed settings. The indoor fan of the RTU is driven by an electronically commutated (EC) motor designed to maintain a constant torque. The outdoor fan of the RTU is driven by an EC motor designed to maintain a constant speed. Both these fan controllers are driven by a pulse-width-modulated (PWM) signal with integer values from 0-100.

4. ***Update charging valve positions.***
   The amount of charge in the system is controlled using this routine. Charge is added or removed using two solenoid valves located on the suction line and liquid line of the RTU, respectively. When charge needs to be added, the low-side solenoid valve is set open; when charge needs to be removed, the high-side solenoid valve is set open. Note that in the initial implementation of the VRC training methodology, charge is only added to the system.

5. ***Read analog temperature and pressure sensor outputs.***
   After the system control set-points have been set to the desired values, the microcontroller reads the current outputs of the thermistors and pressure transducers. The thermistors and pressure transducers output an analog voltage so the built-in analog-to-digital converter (ADC) is used to convert these values to digital inputs.

6. ***Read digital weighing scale output.***
   The amount of refrigerant that has entered the system is measured using a weighing scale with a digital output (via RS-232 serial connection). This routine receives the current output of the weighing scale.

7. ***Send updated measurement values via serial connection.***
   The last process performed by the microcontroller is to send the measured sensor values back to the personal computer via USB serial connection. The output string takes the following form:

```
    ERI_T    SUC_T    DIS_T    CRS_T    CRO_T    SUC_P    DIS_P    CHRG
[   {K},     {K},     {K},     {K},     {K},     {kPa},   {kPa},   {kg},   ]
```

   where

   ERI_T: Evaporator Refrigerant Inlet Temperature, in Kelvin
   SUC_T: Compressor Refrigerant Suction Temperature, in Kelvin
   DIS_T: Compressor Refrigerant Discharge Temperature, in Kelvin
   CRS_T: Condenser Refrigerant Saturation Temperature, in Kelvin
   CRO_T: Condenser Refrigerant Outlet Temperature, in Kelvin
   SUC_P: Compressor Refrigerant Suction Pressure, in kilopascals
   DIS_P: Compressor Refrigerant Discharge Pressure, in kilopascals
   CHRG: Net mass of refrigerant charge, in kilograms.

This procedure is repeated by the microcontroller indefinitely while the training algorithm is being executed. Whenever the control input message is sent from the training kit algorithm (which is once per second) the procedure on the microcontroller is executed and the measurements are sent back in response.

3.2. Training Kit Algorithm Software Implementation Details

An object-oriented implementation of the VRC sensor training algorithm has been implemented and tested. At a high level, the algorithm controls the state of the RTU to a sequence of tests and collected

steady-state data that can be used to tune the empirical parameters used by the VRC sensor. A more thorough description of the important routines and subroutines will be provided in this section. Additionally, flowcharts of the important processes used in the training algorithm are presented in Milestone Report 2.5.a.

On initialization, the training algorithm receives some configuration parameters as inputs and sets up some data connections between the microcontroller and SQLite database used to store the sensor measurements. The serial data connection is initialized by designating the port the microcontroller is connected to and setting the baud rate between the devices. The database connection is simply created by specifying a file path. The schema for storing the data is automatically generated by the training kit object on creation.

Also during initialization, the test sequence is loaded from the configuration file. The test sequence is stored as a list where each element is a list of the desired set-points used for each test. These set-points include the refrigerant charge level, the cooling mode, the indoor fan torque setting, and outdoor fan speed setting. As the algorithm progresses, test scenarios are popped off the list until all the scenarios have been exhausted. At this point, the algorithm has finished testing the system and the RTU is shutdown.

After executing the training algorithm, the software transitions from test scenario to test scenario by applying this sequence of steps. First, the system determines whether the current charge level is at the desired set-point value. If the current charge level is not at the set-point level, the system enters a charge adjustment sequence. In this sequence, the low-side and high-side valves are open or closed in order to add and remove charge respectively. In the initial hardware implementation, only the low-side solenoid valve to add charge was installed. This means that only the addition of charge can be performed, though the logic in the software implementation is the same. This process continues until the charge level reaches the set-point level.

Once the refrigerant charge level has reached the set-point value, the system enters into a steady-state detection state. In this state, the system applies a steady state filter to a fixed length first in, first out (FIFO) buffer of data points. The steady state detector consists of fitting a simple linear regression model to determine the current slope of the sensor measurements in the FIFO buffer. The data contained in this buffer are the sensor outputs and the steady state detector filters each sensor individually. Thus a total of 8 simple linear regression models are determined and the 8 slope estimations are each compared to a threshold value. When the absolute value of the slopes are less than the threshold, and the variance of each sensor data is lower than another threshold, the data are deemed to be steady-state. When the data are not determined to be steady, the process simply waits for more data to enter the FIFO buffer.

When the samples are determined to be steady, the algorithm enters into the steady-state data collection process. This process simply collects steady state data points for a fixed amount of time in order to be used later in the parameter tuning procedure. Currently, 5 minutes' worth of data is

collected at a sampling interval of 1 second. Once 300 samples have been collected, the algorithm exits the current test scenario and begins the process again for the next test scenario.

4. Open Laboratory Training Methodology

The cost and time requirements of testing equipment in psychrometric chamber test facilities to develop empirical models has deterred equipment manufacturers from implementing virtual sensor based FDD methodologies. Currently, equipment manufacturers primarily use psychrometric chambers to perform regulatory equipment ratings tests and to a much lesser extent for developing advanced technologies. To reduce the amount of effort and time required to effectively tune the empirical parameters of the VRC sensor, an algorithm has been proposed that approximates the responses of different charge levels at different ambient conditions without psychrometric chambers. This is accomplished by adjusting the airflow rates through the evaporator and condenser coil in an open laboratory space. This results in the system operating at different low- and high-side pressures for a given level of charge, shown in Figure 4.1. By also changing the amount of refrigerant charge in the system, the response of charge level on suction superheat, liquid-line subcooling, and evaporator refrigerant inlet quality can be observed at different operating conditions.

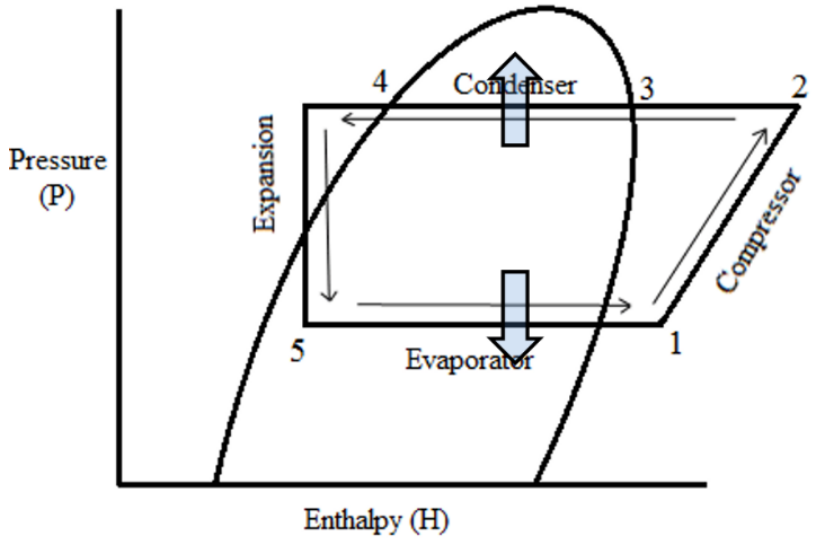

Figure 4.1. When evaporator and condenser airflow rates are reduced, the evaporating and condensing pressure are respectively decreased and increased.

In BP4, a methodology to tune the empirical VRC sensor parameters in open laboratory testing was developed. This method involved manually controlling the fan speeds and adding refrigerant to the system. To further improve this methodology, an automated open laboratory VRC training system has been developed.

When the automated open laboratory VRC training system is applied to the RTUs, the operational state of the RTU is automatically controlled to 38 different combinations of charge level, cooling stage, indoor fan torque, and outdoor fan torque. Each of these test combinations is shown in

Table 4.1. The test conditions in

Table 4.1 were selected by determining the optimal fan settings in the open laboratory to train a model that minimizes the error using psychrometric chamber test data. Despite having 38 test conditions, the entire sequence is completed within 8-12 hours, or approximately 15 minutes per test.

Table 4.1. Optimal sequence of test conditions used in automated VRC sensor training algorithm.

Test	Charge Level[1] [%]	Compressor Stage [-]	Indoor Fan Torque[2] [%]	Outdoor Fan Torque[3] [%]
1	60	LOW	60	70
2	60	LOW	60	40
3	60	LOW	30	40
4	60	LOW	30	70
5	60	HIGH	90	100
6	60	HIGH	90	70
7	60	HIGH	50	70
8	60	HIGH	50	100
9	70	LOW	60	70
10	70	LOW	30	40
11	70	HIGH	90	100
12	70	HIGH	50	70
13	80	LOW	60	70
14	80	LOW	30	40
15	80	HIGH	90	100
16	80	HIGH	50	70
17	90	LOW	60	70
18	90	LOW	30	40
19	90	HIGH	90	100
20	90	HIGH	50	70
21	100	LOW	60	70
22	100	LOW	60	40
23	100	LOW	30	40
24	100	LOW	30	70
25	100	HIGH	90	100
26	100	HIGH	90	70
27	100	HIGH	50	70
28	100	HIGH	50	100
29	110	LOW	60	70
30	110	LOW	30	40
31	110	HIGH	90	100
32	110	HIGH	50	70
33	120	LOW	60	70
34	120	LOW	30	40
35	120	HIGH	90	100
36	120	HIGH	50	70

[1] Charge is measured relative to the recommended charge according to the manufacturer's nameplate data.
[2] Indoor fan torque is set according to a nominal flow rate of 1350 CFM for low stage operation and 2000 CFM for high stage operation.
[3] Outdoor fan torque is set using the manufacturer's default values for low and high stage operation.

Initially, the rated parameters used in the VRC sensor model (Equation 1.3) were determined using the open laboratory training data. However, after assessing the performance of the tuned VRC models it was noticed that significant biases often resulted when compared to the test data. It was determined that the rated parameters used in the empirical model strongly influenced these biases. In order to overcome this issue and to avoid doing additional psychrometric chamber testing, the empirical rating parameters were determined using optimization. To optimize these parameters, first least-squares regression is applied to the open laboratory training data to determine k_{sh}, k_{sc}, k_x using initial guess values for $\Delta T_{sh,rated}$, $\Delta T_{sc,rated}$, and $x_{eri,rated}$. Following this, values for $\Delta T_{sh,rated}$, $\Delta T_{sc,rated}$, and $x_{eri,rated}$ are set to the values measured for one of the test conditions of the AHRI ratings test that result in the least mean-square-error for normal charge levels. The AHRI ratings tests used A_1, A_2, B_1, and B_2 specified in AHRI Standard 210/240. The procedure could be generalized by including all of the steady-state ratings tests prescribed by equipment rating protocols. This procedure resulted in better charge level estimates applied to the psychrometric chamber validation data.

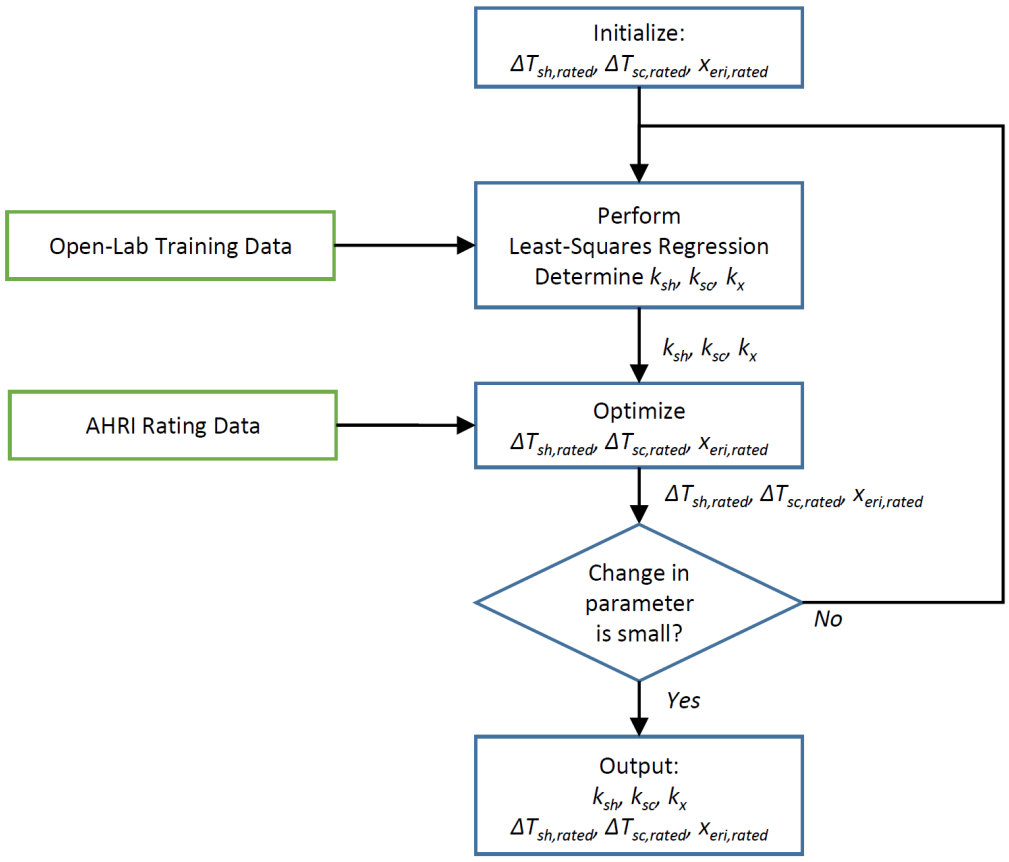

Figure 4.2. Procedure used to determine empirical parameters used in the VRC sensor using open laboratory training data and AHRI Ratings test data.

In order to test the performance of the automated VRC sensor training algorithm and virtual sensor implementation, a series of tests were performed. The test plan had two primary considerations in

mind: evaluate how well the open laboratory training algorithm tunes the empirical VRC parameters and how well the VRC sensor performs for different types of systems. To do this, combinations of different expansion valves and condenser coils were used in a 5-ton RTU as described in Table 4.2. The RTU has two cooling stages, a variable speed indoor blower, and a variable speed outdoor fan.

Table 4.2. System configurations and testing environments planned to evaluate automated virtual sensor training algorithm and virtual charge sensor performance.

ID	Expansion Device	Condenser Coil	Test Environment
A2[1]	TXV	Microchannel	Psychrometric Chamber Testing
A1[1]	TXV	Microchannel	Automated Open Lab Training
B1[1]	FXO	Microchannel	Automated Open Lab Training
B2	FXO	Microchannel	Psychrometric Chamber Testing
C1[2]	FXO	Finned-Tube	Automated Open Lab Training
C2	FXO	Finned-Tube	Psychrometric Chamber Testing
D1[2]	TXV	Finned-Tube	Automated Open Lab Training
D2	TXV	Finned-Tube	Psychrometric Chamber Testing

[1] Tests were completed during BP4 or earlier in BP5.
[2] Testing for C1 and D1 will be performed inside the psychrometric chambers simulating an open laboratory space. This will be done in order to accelerate the tests by not having to remove the RTU from the psychrometric chamber facility once it has been installed.

5. Psychrometric Chamber Test Results

In an effort to assess the accuracy of the VRC sensor applied to different types of RTUs, extensive testing within psychrometric chambers has been performed.

The first system tested in the psychrometric chamber test facilities was System A (microchannel condenser, thermostatic expansion valve). The empirical parameters of the VRC model were determined using the automated open laboratory training kit. The RTU was installed in the psychrometric chamber test facilities and was tested for both stages of cooling. These test conditions are described in Table 5.1 for low stage and Table 5.2 for high stage.

Table 5.1. Test conditions for RTU with microchannel condenser and thermostatic expansion valve (System A) for low stage cooling operation in psychrometric test chambers.

Test Variable		Test Values
Compressor Stage	[-]	LOW
Indoor Dry Bulb	[°F]	80
Indoor Wet Bulb	[°F]	67
Outdoor Dry Bulb	[°F]	69, 82, 95
Charge Level[1]	[%]	60, 70, 80, 90, 100, 110, 120
Indoor Fan Torque[2]	[%]	40, 60
Outdoor Fan Torque[3]	[%]	40, 70

[1] Charge is measured relative to the recommended charge according to the manufacturer's nameplate data.
[2] Indoor fan torque is set according to a nominal flow rate of 1350 CFM for low stage operation.

[3] Outdoor fan torque is set using the manufacturer's default value for low stage operation.

Table 5.2. Test conditions for RTU with microchannel condenser and thermostatic expansion valve (System A) for high stage cooling operation in psychrometric test chambers.

Test Variable		Test Values
Compressor Stage	[-]	HIGH
Indoor Dry Bulb	[°F]	80
Indoor Wet Bulb	[°F]	67
Outdoor Dry Bulb	[°F]	82, 95, 108
Charge Level[1]	[%]	60, 70, 80, 90, 100, 110, 120
Indoor Fan Torque[2]	[%]	60, 90
Outdoor Fan Torque[3]	[%]	70, 100

[1] Charge is measured relative to the recommended charge according to the manufacturer's nameplate data.
[2] Indoor fan torque is set according to a nominal flow rate of 2000 CFM for high stage operation.
[3] Outdoor fan torque is set using the manufacturer's default value for high stage operation.

The resulting accuracy of the VRC sensor models trained in the open laboratory space and applied to the psychrometric chamber test data collected over the range of ambient conditions is shown for both cooling stages in Figure 5.1. The results show that the VRC sensor outputs for low-stage cooling tests were less accurate than those for high-stage cooling operation. This trend was observed for the other systems as well. At low charge levels, the performance of the VRC sensor during low-stage operation was worse. It can be seen that even the training data were less accurately predicted at low charge levels. This was not the case for high stage cooling operation; the accuracy was relatively the same at all charge levels tested. It should be noted that the root-mean-squared error (RMSE) was less than 10% for both stages of operation. This indicates that the predictions from the VRC sensor could be used as part of an automated FDD system with relative confidence.

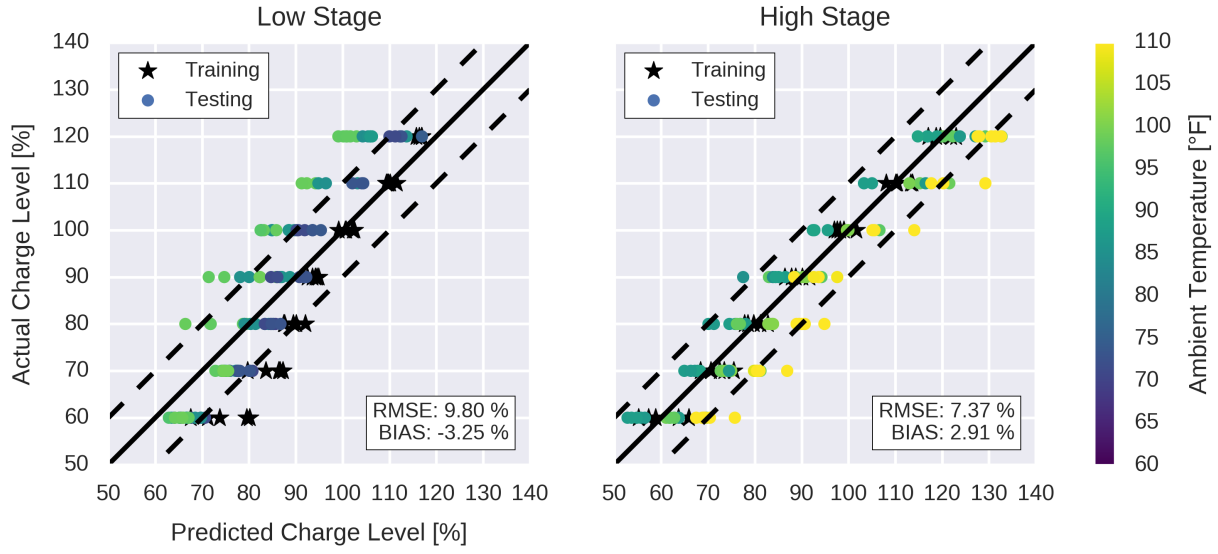

Figure 5.1. VRC sensor prediction accuracy for RTU with microchannel condenser and thermostatic expansion valve (System A) applied to both stages of operation under different ambient conditions.

After the completion of testing and evaluating the data collected from System A, the thermostatic expansion valve (TXV) was replaced by a fixed orifice expansion device. The orifice size and design was selected with the help of the original equipment manufacturer to ensure that the performance of the unit was representative of actual units. After the replacement of the expansion device, the RTU was referenced as System B.

The automated open laboratory training kit was applied to System B in an open laboratory space in order to collect data used to determine the empirical parameters of the VRC sensor model. At the conclusion of this process, the RTU was installed in the psychrometric chambers and tested over a range of ambient conditions. The test conditions for low-stage and high-stage operation are described in Table 5.3 and Table 5.4, respectively. These conditions were similar to those tested for System A, but extended to include the high temperature condition during low stage operation and the cool temperature condition during high stage operation.

Table 5.3. Test conditions for RTU with microchannel condenser and fixed orifice expansion device (System B) for low stage cooling operation in psychrometric test chambers.

Test Variable		Test Values
Compressor Stage	[-]	LOW
Indoor Dry Bulb	[°F]	80
Indoor Wet Bulb	[°F]	67
Outdoor Dry Bulb	[°F]	69, 82, 95, 108
Charge Level[1]	[%]	60, 70, 80, 90, 100, 110, 120
Indoor Fan Torque[2]	[%]	40, 60
Outdoor Fan Torque[3]	[%]	40, 70

[1] Charge is measured relative to the recommended charge according to the manufacturer's nameplate data.
[2] Indoor fan torque is set according to a nominal flow rate of 1350 CFM for low stage operation.
[3] Outdoor fan torque is set using the manufacturer's default value for low stage operation.

Table 5.4. Test conditions for RTU with microchannel condenser and fixed orifice expansion device (System B) for high stage cooling operation in psychrometric test chambers.

Test Variable		Test Values
Compressor Stage	[-]	HIGH
Indoor Dry Bulb	[°F]	80
Indoor Wet Bulb	[°F]	67
Outdoor Dry Bulb	[°F]	69, 82, 95, 108
Charge Level[1]	[%]	60, 70, 80, 90, 100, 110, 120
Indoor Fan Torque[2]	[%]	60, 90
Outdoor Fan Torque[3]	[%]	70, 100

[1] Charge is measured relative to the recommended charge according to the manufacturer's nameplate data.
[2] Indoor fan torque is set according to a nominal flow rate of 2000 CFM for high stage operation.
[3] Outdoor fan torque is set using the manufacturer's default value for high stage operation.

The accuracy of the VRC sensor models for System B trained using open laboratory data and applied to the psychrometric chamber test data collected over the range of ambient conditions is shown for both cooling stages in Figure 5.2. The results show that the low-stage cooling test VRC predictions were less accurate than those for high-stage cooling operation. This is especially true when the amount of

refrigerant charge was above 90%. After analysis of the experimental data, it was determined that for these cases, the system operated with zero superheat or subcooling. One explanation for this is the diameter of the fixed orifice was too large for the low-stage operation. This is understandable since the orifice must be designed for the high stage operation in order to maximize design point performance. Because there was no superheat or subcooling for these conditions, the VRC model must rely entirely on the evaporator refrigerant quality term (which is essentially a function of condensing pressure). With this in mind, the performance of the VRC sensor is rather respectable considering the system performance information available. The RMSE error for the low stage operation was on par with the results obtained for System A. The accuracy during high stage operation was actually better than System A at 6.68%.

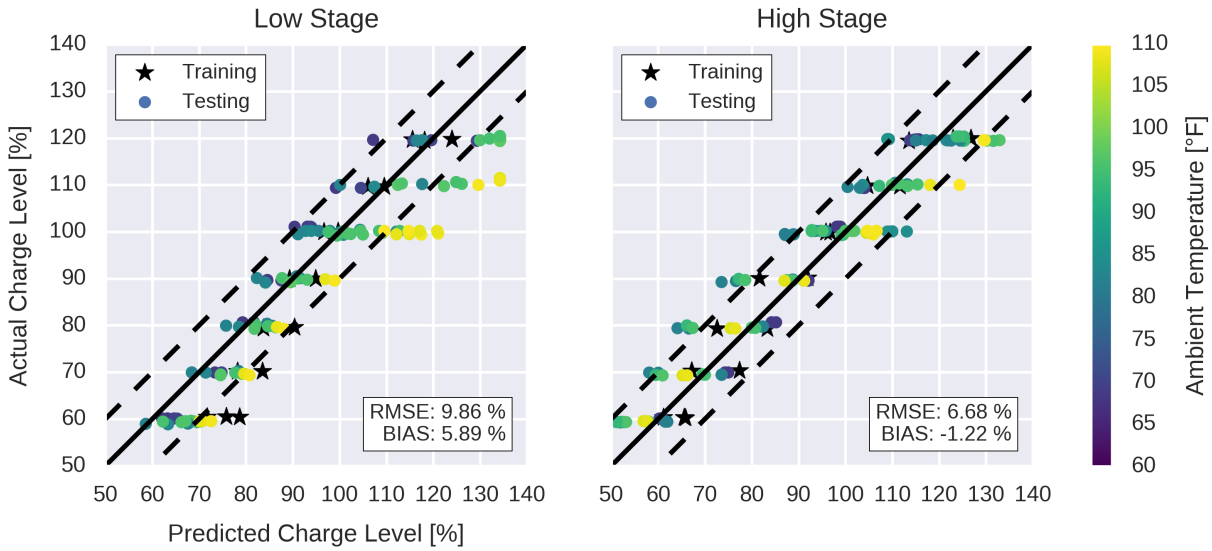

Figure 5.2. VRC sensor prediction accuracy for RTU with microchannel condenser and fixed orifice expansion device (System B) applied to both stages of operation under different ambient conditions.

Following the testing and evaluation of the data collected from System B, the microchannel condenser coil originally installed on the unit was replaced by a finned tube condenser coil received from the original equipment manufacturer. This coil was designed for the RTU and can be ordered as a lower efficiency option. After the replacement of the condenser coil, the RTU was referenced as System C.

Because the system was already installed in the psychrometric chambers at this point, the open laboratory training kit was applied with the system installed in the psychrometric chambers rather than the open laboratory space. Open laboratory space conditions were simulated by controlling the air entering the evaporator and condenser coils to be equal at typical indoor conditions. One advantage of this was that the environmental conditions used to train the VRC sensor could be analyzed and its impact on the accuracy of the VRC model assessed.

Following the training tests, System C was tested in the psychrometric chambers over a wide range of ambient conditions. The conditions tested for low and high stage operation are described in Table 5.5 and Table 5.6, respectively. These test conditions were expanded from System B since the testing was progressing ahead of schedule, including testing at both wet and dry coil conditions for a subset of tests.

Table 5.5. Test conditions for RTU with finned-tube condenser and fixed orifice expansion device (System C) for low stage cooling operation in psychrometric test chambers.

Test Variable		Test Values
Compressor Stage	[-]	LOW
Indoor Dry Bulb	[°F]	80
Indoor Wet Bulb	[°F]	57, 67
Outdoor Dry Bulb	[°F]	67, 82, 95, 108
Charge Level[1]	[%]	60, 70, 80, 90, 100, 110, 120
Indoor Fan Torque[2]	[%]	30, 60
Outdoor Fan Torque[3]	[%]	40, 70

[1] Charge is measured relative to the recommended charge according to the manufacturer's nameplate data.
[2] Indoor fan torque is set according to a nominal flow rate of 1350 CFM for low stage operation.
[3] Outdoor fan torque is set using the manufacturer's default value for low stage operation.

Table 5.6. Test conditions for RTU with finned-tube condenser and fixed orifice expansion device (System C) for high stage cooling operation in psychrometric test chambers.

Test Variable		Test Values
Compressor Stage	[-]	HIGH
Indoor Dry Bulb	[°F]	80
Indoor Wet Bulb	[°F]	57, 67
Outdoor Dry Bulb	[°F]	69, 82, 95, 108
Charge Level[1]	[%]	60, 70, 80, 90, 100, 110, 120
Indoor Fan Torque[2]	[%]	50, 90
Outdoor Fan Torque[3]	[%]	70, 100

[1] Charge is measured relative to the recommended charge according to the manufacturer's nameplate data.
[2] Indoor fan torque is set according to a nominal flow rate of 2000 CFM for high stage operation.
[3] Outdoor fan torque is set using the manufacturer's default value for high stage operation.

The accuracy of the VRC model designed for System C for each stage of operation is shown in Figure 5.3 over the range of ambient conditions tested. The performance of the VRC sensor applied to System C was better than System A or System B, which may indicate that a system having a finned tube condenser may be modeled more easily. In both stages of operation, the RMSE was approximately 6.20%. Additionally, the accuracy observed over the range of charge levels was relatively constant.

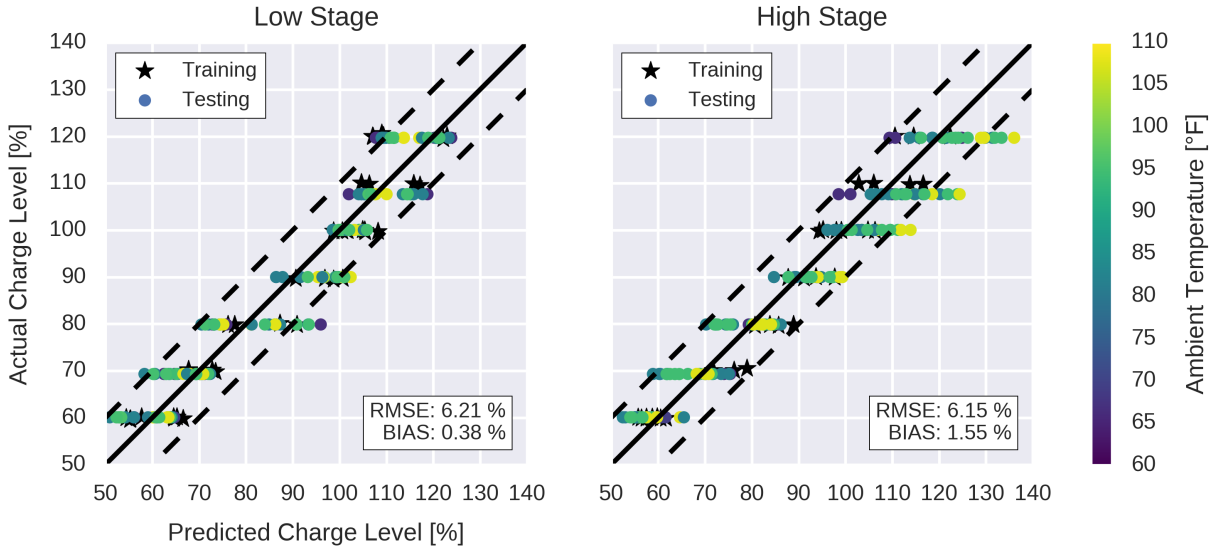

Figure 5.3. VRC sensor prediction accuracy for RTU with finned tube condenser and fixed orifice expansion device (System C) applied to both stages of operation under different ambient conditions.

After the testing and evaluating the data for System C, the fixed orifice valve was replaced by a thermostatic expansion valve (TXV). The new system is referenced as System D. Again, as the unit was already inside the Psychrometric chamber, open laboratory space conditions were simulated by controlling the air entering the evaporator and condenser coils to be equal at typical indoor conditions. After the training, System D was tested and data was collected at all conditions similar to those of System C. Table 5.7 and Table 5.8 summarize all the test conditions for System D which includes dry-coil as well as wet-coil conditions.

Table 5.7. Test conditions for RTU with finned-tube condenser and thermostatic expansion valve (System D) for low stage cooling operation in psychrometric test chambers.

Test Variable		Test Values
Compressor Stage	[-]	LOW
Indoor Dry Bulb	[°F]	80
Indoor Wet Bulb	[°F]	57, 67
Outdoor Dry Bulb	[°F]	67, 82, 95, 108
Charge Level[1]	[%]	60, 70, 80, 90, 100, 110, 120
Indoor Fan Torque[2]	[%]	30, 60
Outdoor Fan Torque[3]	[%]	40, 70

[1] Charge is measured relative to the recommended charge according to the manufacturer's nameplate data.
[2] Indoor fan torque is set according to a nominal flow rate of 1350 CFM for low stage operation.
[3] Outdoor fan torque is set using the manufacturer's default value for low stage operation.

Table 5.8. Test conditions for RTU with finned-tube condenser and thermostatic expansion valve (System D) for high stage cooling operation in psychrometric test chambers.

Test Variable		Test Values
Compressor Stage	[-]	HIGH
Indoor Dry Bulb	[°F]	80
Indoor Wet Bulb	[°F]	57, 67
Outdoor Dry Bulb	[°F]	69, 82, 95, 108
Charge Level[1]	[%]	60, 70, 80, 90, 100, 110, 120
Indoor Fan Torque[2]	[%]	50, 90
Outdoor Fan Torque[3]	[%]	70, 100

[1] Charge is measured relative to the recommended charge according to the manufacturer's nameplate data.
[2] Indoor fan torque is set according to a nominal flow rate of 2000 CFM for high stage operation.
[3] Outdoor fan torque is set using the manufacturer's default value for high stage operation.

The accuracy of the VRC model designed for System D for each stage of operation is shown in Figure 5.4 over the range of ambient conditions tested. The RMSE was approximately 6.66% for low stage operation, while for the high stage it was around 5.71%.

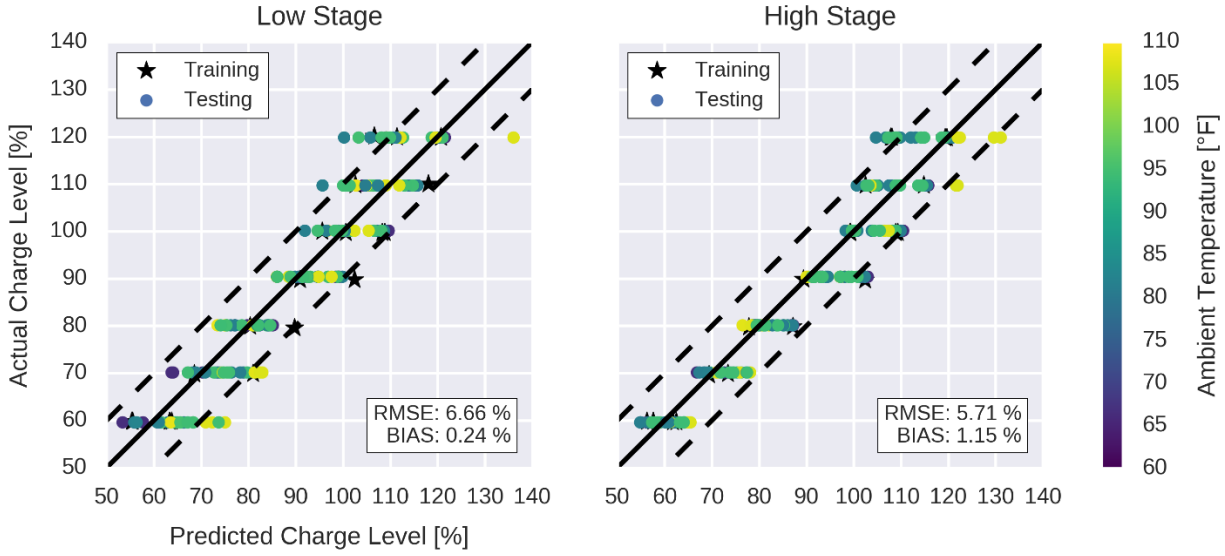

Figure 5.4. VRC sensor prediction accuracy for RTU with finned tube condenser and thermostatic expansion valve (System D) applied to both stages of operation under different ambient conditions.

The accuracy of the VRC models developed for the four systems tested are shown together in Table 5.9. For all systems, both the RMSE at each stage and the overall accuracy were less than the goal of 10%. For the microchannel units, the VRC sensor is less accurate during low stage operation. For these systems, the subcooling was very sensitive to the charge level. This often led to zero subcooling at many test conditions. Furthermore, when these systems were overcharged, superheat was driven to zero. This made estimating the refrigerant charge level problematic using the proposed model. The results

also show that the open laboratory training algorithm provides experimental data that can be used to design VRC models without extensive testing in psychrometric chamber test facilities.

Table 5.9. Summary of the prediction accuracy of the VRC sensor applied to the different systems tested during this study.

System	Expansion Device	Condenser Coil	RMSE (%)		
			Low Stage	High Stage	Overall
A	TXV	Microchannel	9.80	7.37	8.56
B	FXO	Microchannel	9.86	6.68	8.27
C	FXO	Finned-Tube	6.21	6.15	6.18
D	TXV	Finned-Tube	6.66	5.71	6.19

6. Conclusions

A methodology and system have been implemented to automatically tune the empirical parameters of a virtual sensor for estimating the amount of refrigerant in an RTU. This system reduces engineering time and costs associated with the virtual sensor by reducing the number of tests required for training, eliminating the need for psychrometric room testing by using open laboratory testing instead, and automating the process of changing charge and refrigerant conditions. In order to assess the accuracy of this methodology, the system was applied to four different RTUs (with varying types of components). The resulting model was then compared with data collected from tests using psychrometric chamber facilities over a wide range of ambient conditions. The results showed that the overall accuracy of each of the virtual refrigerant charge sensor models had root-mean-square errors less than 10%. This shows that the automated open laboratory training system results in accurate sensors for many types of RTUs.

After analyzing the data, it was observed that the VRC sensor tends to be less accurate when applied to systems with microchannel condensers. While the reasons for this loss of accuracy are somewhat unclear, it may be caused by the much smaller condenser volume in comparison to systems with conventional finned tube condensers. The systems that were tested with microchannel condensers tended to have lower levels of subcooling as well, especially for low charge levels. Since subcooling is an essential input to the VRC sensor, accurate prediction of charge levels is much more difficult when subcooling is zero at undercharged conditions. Further investigation of systems with microchannel would provide more evidence and possibilities for improvement in the VRC sensor model.

One of the most significant impact of this project is believed to be the automated equipment testing. The benefits of automating the equipment operation during the laboratory testing were greater than initially expected. Many more tests were completed than originally expected with much less time and effort. In the future, it may be possible to generate improved equipment performance models as well as implement automated load-based testing to test the performance of system with variable speed equipment. Reducing performance testing effort and requirements has the potential to save significant development costs which could accelerate the technological improvement in direct-expansion air conditioning and refrigeration equipment.